

Structure of Large ${}^3\text{He}$ - ${}^4\text{He}$ Mixed Drops around a Dopant Molecule

Martí Pi, Ricardo Mayol, and Manuel Barranco

Departament ECM, Facultat de Física, Universitat de Barcelona, E-08028 Barcelona, Spain

(Received 24 November 1998)

We have investigated how helium atoms are distributed within a mixed ${}^3\text{He}_{N_3}$ - ${}^4\text{He}_{N_4}$ large drop with $N_3 \gg N_4$. For drops doped with a SF_6 molecule or a Xe atom, we have found that the number of ${}^3\text{He}$ atoms within the volume containing the first two solvation shells increases when N_4 decreases in such a way that these dopants may be in a superfluid environment for $N_4 \geq 60$, which gradually disappears as N_4 decreases. The result is in qualitative agreement with recent experimental data. [S0031-9007(99)08864-X]

PACS numbers: 67.60.-g, 36.40.-c

In a recent experiment, Grebenov *et al.* [1] have carried out the equivalent of the Andronikashvili experiment [2] in a microscopic system, namely, a mixed ${}^3\text{He}$ - ${}^4\text{He}$ drop consisting of about 10^4 atoms doped with an oxygen carbon sulfide (OCS) molecule. By analyzing the infrared spectrum of OCS, Grebenov *et al.* (see also Ref. [3]) conclude that the molecule freely rotates when a number of ${}^4\text{He}$ atoms large enough coat the impurity, preventing the ${}^3\text{He}$ atoms, which are in the normal phase at a temperature of the order of 150 mK [4,5], from getting too close to the OCS molecule. That number is of the order of 60, in excellent agreement with path integral [6] and variational [7] Monte Carlo calculations. It is remarkable that the presence of the impurity, which causes the ${}^4\text{He}$ density to rise up to several times the saturation value, is not destroying its superfluid character, and that, in spite of the high densities reached, the first solvation shell remains liquid [8]. An indication of this fluidlike behavior is that the peak density in the first solvation shell continues to increase as the second shell grows [9].

Even if the interpretation of the microscopic Andronikashvili experiment is on a firm basis, a remaining major question is how ${}^3\text{He}$ is distributed around the ${}^4\text{He}$ -plus-impurity complex, and, in general, how liquid ${}^3\text{He}$ is dissolved into ${}^4\text{He}$ droplets at very low temperatures. These are the questions we want to address in this paper.

At zero temperature, it is known that the maximum solubility of ${}^3\text{He}$ in the bulk of ${}^4\text{He}$ is $\sim 6.6\%$ [10]. For liquid ${}^4\text{He}$ systems having a free surface, it is also known that a large amount of ${}^3\text{He}$ is accumulated on the free surface occupying Andreev states [11,12] before it starts being dissolved into the bulk. In the case of drops made of up to several thousand atoms, the surface region constitutes a sizeable part of the system [13], and the surface has a large capacity for storing ${}^3\text{He}$ atoms before they get inside the drop [14]. Because of the wide free surface of both isotopes [15,16] and the low surface tension of the ${}^3\text{He}$ - ${}^4\text{He}$ liquid interface [17], one expects that this region plays a prominent role when it constitutes a large part of the system or, as in the present case, when it is close to the dopant atom or molecule.

The structure and energetics of mixed, doped or not, helium droplets have been addressed using a finite-range density functional method [14]. That work was carried out before the experiments reported in Ref. [1], and the emphasis was put on improving the density functional method to better describe the thermodynamical properties of the liquid mixture, and to study rather small mixed droplets with $N_4 \gg N_3$. Our main goal here is to apply the density functional method to droplets whose characteristics are closer to those of the experiments, with the restriction of spherical symmetry for the He-impurity potential for the sake of simplicity. We have considered Xe and SF_6 as dopants, using for the latter a spherically averaged interaction potential. The Xe-He potential is weaker than the SF_6 -He potential. In this respect, our results for that atomic impurity should better represent the experimental ones for OCS even if this linear molecule produces deformations in the helium drop that we have not considered here. The density functional method and the treatment of the impurity are thoroughly described in Ref. [14].

The large number of ${}^3\text{He}$ atoms in the droplets we are describing ($N_3 > 1000$) allows us to employ an extended Thomas-Fermi method to describe the fermionic component of the mixture. We have used for the ${}^3\text{He}$ kinetic energy density the expression given in Ref. [18], which contains up to second order density gradient corrections to the standard $\sim \rho_3^{5/3}(r)$ expression, where ρ_3 and ρ_4 will denote the particle density of each isotope. We have checked that this density functional reproduces accurately the Hartree-Fock results [14] obtained for the largest drops studied (see also Refs. [5,18]).

Figure 1 displays the situation in which a ${}^4\text{He}_{728}$ drop, whose size is large enough to clearly distinguish in it a surface and bulk region, is coated with an increasing number of ${}^3\text{He}$ atoms, and the limiting situation of the same drop immersed into liquid ${}^3\text{He}$. The evolution with N_3 of the ${}^3\text{He}$ concentration inside the ${}^4\text{He}$ drop, defined as $x_3 \equiv \rho_3/(\rho_4 + \rho_3)|_{\text{bulk}}$, is shown in the inset of Fig. 1. Several interesting features of this figure are worth comment. A fairly large amount of ${}^3\text{He}$ is needed before it is appreciably dissolved in the bulk: For $N_3 = 1000$,

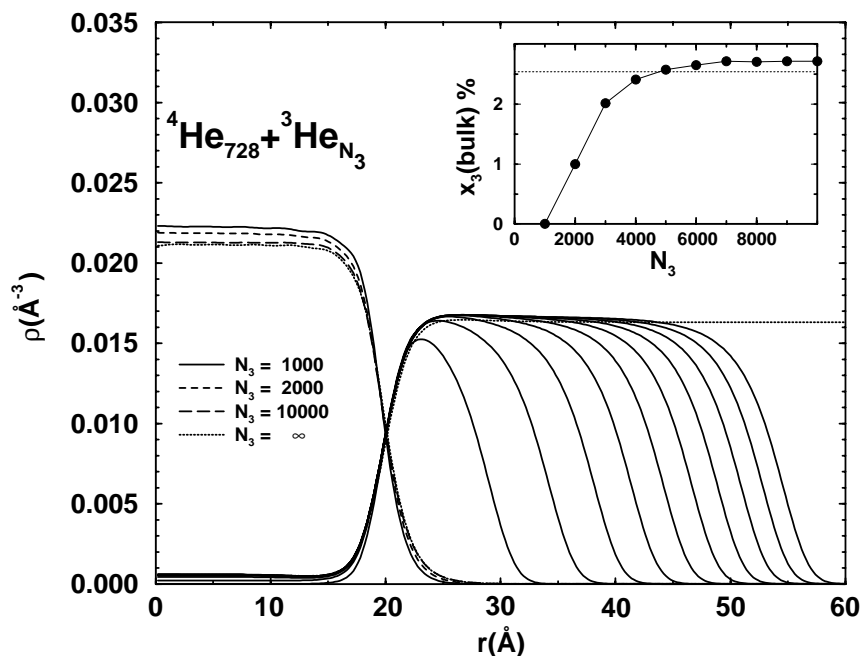


FIG. 1. Density profiles of ${}^4\text{He}_{728} + {}^3\text{He}_{N_3}$ droplets for N_3 values from 1000 to 10000 in $\Delta N_3 = 1000$ steps. For clarity, only the ${}^4\text{He}$ densities corresponding to a few N_3 cases have been plotted. Also shown is the density profile of a ${}^4\text{He}_{728}$ drop immersed into liquid ${}^3\text{He}$ (dotted lines). Inset: Bulk ${}^3\text{He}$ concentrations. The connecting solid line is to guide the eye. Also shown is the value corresponding to ${}^4\text{He}_{728}$ in liquid ${}^3\text{He}$ (dotted line).

ρ_3 near the origin is $\sim 1.4 \times 10^{-8} \text{\AA}^{-3}$. The solubility is appreciably reduced by finite size effects. Indeed, one can see from the inset that the limiting solubility in the $N_4 = 728$ drop is $\sim 2.5\%$, as compared to the 6.6% value in the liquid mixture. It is also worth noting that, for large N_3 droplets, the bulk solubility is slightly higher than the limiting solubility, indicating that finite size effects still appear in rather large drops. Another manifestation of a finite size effect is that the average ${}^3\text{He}$ density is above the saturation value even for the larger drops, showing that the existence of the outer ${}^3\text{He}$ surface still causes a visible density compression.

Because of the high incompressibility of helium, the bulk density of ${}^4\text{He}$ decreases when ${}^3\text{He}$ is dissolved, and the rms radius of the ${}^4\text{He}$ drop manifests a peculiar N_3 behavior. It decreases when N_3 increases up to a few hundreds due to the initial compression of the outermost ${}^4\text{He}$ surface, and then steadily increases as ${}^4\text{He}$ is pushed off the center by intruder ${}^3\text{He}$ atoms. This is a very tiny effect anyway. For example, we have found that the rms radius of the ${}^4\text{He}_{728}$ drop is 15.70 \AA . It decreases when ${}^3\text{He}$ is added, reaching a minimum value of 15.64 \AA for $N_3 \sim 250$, and then it steadily increases up to 16.11 \AA for $N_3 = 10000$. The rms radius of the ${}^4\text{He}_{728}$ drop immersed into liquid ${}^3\text{He}$ is 16.14 \AA .

When a SF_6 molecule is captured by a helium drop, it moves into the bulk, producing a drastic rearrangement of the drop density around it [19–22]. For large ${}^4\text{He}$ droplets, the appearance of two high density solvation

shells with a density-depleted region in between is especially noteworthy. It is then natural to ask about the possible existence of Andreev-like states arising at the “inner ${}^4\text{He}$ surface,” and whether a large number of ${}^3\text{He}$ atoms can be stored there, producing an “onion”-like structure of alternative ${}^4\text{He}$ and ${}^3\text{He}$ shells around the impurity, or even when $N_3 \gg N_4$, the latter can displace the former in the first solvation shell.

Figure 2 shows the density profiles of several ${}^4\text{He}_{728} + {}^3\text{He}_{N_3} + \text{SF}_6$ droplets, giving a positive answer to the first question and a negative answer to the other two. We have found that, indeed, about *one* ${}^3\text{He}$ atom is in the inner surface, but that ${}^3\text{He}$ mostly coats the ${}^4\text{He}$ -plus-impurity complex, as in undoped droplets. To check this result we have started the calculations from different initial shapes, some having the “onion”-like form mentioned earlier. It has turned out that these are always high energy, metastable configurations, and the mixed droplet eventually evolves towards stable configurations of the type shown in Fig. 2. The larger zero point motion energy of ${}^3\text{He}$ makes it energetically more advantageous to fill the first solvation shell with ${}^4\text{He}$ atoms, and ${}^3\text{He}$ is expelled to the outer region of the drop.

We are now in a position to discuss a physical situation relevant to the microscopic Andronikashvili experiment. We observe that the first solvation shell [23] can host ~ 23 ${}^4\text{He}$ atoms in the case of SF_6 as a dopant, and ~ 15 atoms in the case of Xe [19–21]. According to Refs. [6–8], these numbers are too small for the ${}^4\text{He}$

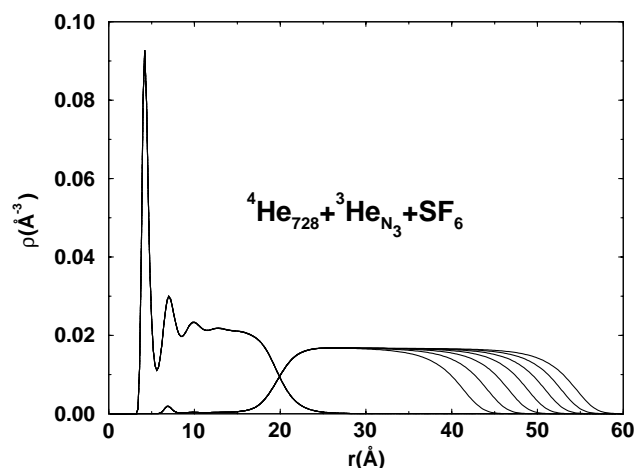


FIG. 2. Density profiles of ${}^4\text{He}_{728} + {}^3\text{He}_{N_3} + \text{SF}_6$ droplets for for N_3 values from 4000 to 10000 in $\Delta N_3 = 1000$ steps.

droplet being superfluid. It is thus crucial to know how the second solvation shell is built, especially what is its composition. Too many ${}^3\text{He}$ atoms in that shell might shrink or even wash out the superfluid environment around the dopant. The density functional method cannot tell whether a given configuration is superfluid or not, but it can give a quantitative answer to its local composition because it is able to reproduce available microscopic density profiles [19,20,24]. We present examples of such compositions in Figs. 3 and 4.

Figure 3 shows the density profiles for ${}^4\text{He}_{N_4} + {}^3\text{He}_{1000} + \text{SF}_6$ and ${}^4\text{He}_{N_4} + {}^3\text{He}_{1000} + \text{Xe}$ with $N_4 = 35, 60,$ and 100 . We have carried out calculations for two different dopants to ascertain the influence of the He-impurity potential on the results. It turns out that a weaker attractive potential favors the mixing of both isotopes in the whole allowed volume (the Xe-He and SF_6 -He potentials are plotted in Ref. [21], for instance). However, this is in part a first glance effect, since the number of ${}^3\text{He}$ atoms in the first solvation shell around Xe is less than 1 (see Fig. 4). Rather, the relevance of Fig. 3 lies in that it shows how ${}^3\text{He}$ is filling the second solvation shell as N_4 decreases.

A more quantitative look at this phenomenon is presented in Fig. 4, where we have plotted the number of atoms of each isotope as a function of the radial distance to the center of the drop. Notice that for a given impurity, the number of ${}^4\text{He}$ atoms in the first solvation shell (extending up to ~ 5.5 Å) is sensibly the same for the three selected N_4 values. It is also worth looking at the ratios $N_3/(N_4 + N_3)$ within the second solvation shell which extend from ~ 5.5 to ~ 8.5 Å. In the SF_6 case, they are $\sim 8\%$ for $N_4 = 100$, $\sim 29\%$ for $N_4 = 60$, and $\sim 65\%$ for $N_4 = 35$. Considering the content of the two shells, these ratios are $\sim 5\%$, $\sim 19\%$, and $\sim 41\%$ which correspond, respectively, to 3, 10, and 22 ${}^3\text{He}$ atoms. The values for Xe are slightly smaller. These numbers make it quite plausible that a SF_6

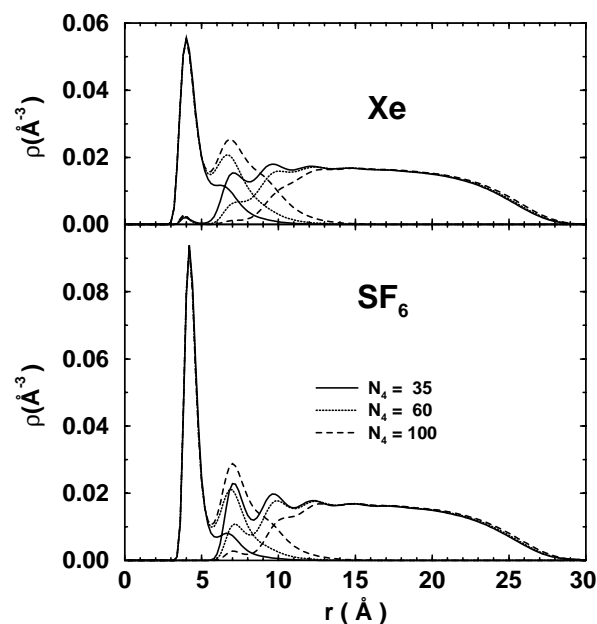


FIG. 3. Bottom panel: Density profiles of ${}^4\text{He}_{N_4} + {}^3\text{He}_{1000} + \text{SF}_6$ droplets for $N_4 = 35, 60,$ and 100 . Top panel: Density profiles of ${}^4\text{He}_{N_4} + {}^3\text{He}_{1000} + \text{Xe}$ droplets for the same N_4 values.

molecule or a Xe atom in a ${}^4\text{He}_{N_4} + {}^3\text{He}_{1000}$ drop is in a superfluid environment when $N_4 = 100$ or 60 , whereas it is not when $N_4 = 35$, as the microscopic Andronikashvili experiment indicates for OCS.

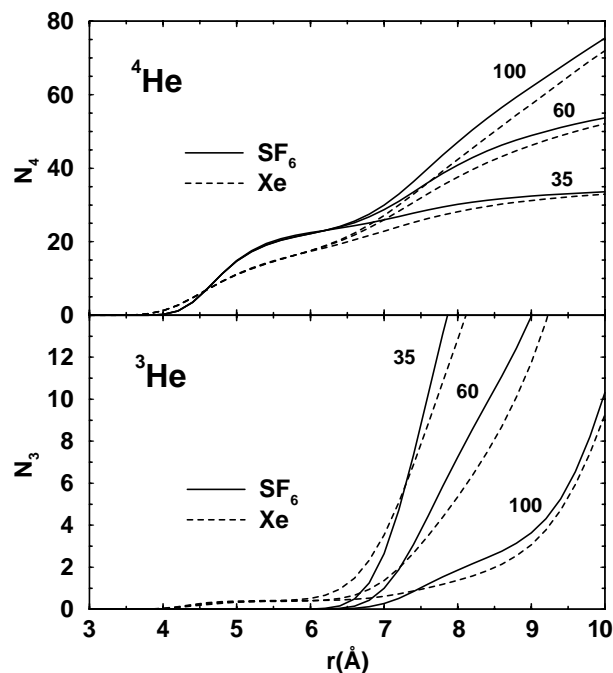


FIG. 4. Top panel: Number of ${}^4\text{He}$ atoms as a function of the radial distance for the droplets of Fig. 3. Bottom panel: Number of ${}^3\text{He}$ atoms as a function of the radial distance for the same droplets.

We are indebted to Peter Toennies and Andrej Vilesov for useful discussions. This work has been performed under Grants No. PB95-1249 and No. PB95-0271-C02-01 from CICYT, Spain, and Program No. 1998SGR-00011 from Generalitat of Catalunya.

-
- [1] S. Grebenev, J.P. Toennies, and A.F. Vilesov, *Science* **279**, 2083 (1998).
- [2] E.L. Andronikashvili, *J. Phys. USSR* **10**, 201 (1946).
- [3] K.K. Lehmann and G. Scoles, *Science* **279**, 2065 (1998).
- [4] D.M. Brink and S. Stringari, *Z. Phys. D* **15**, 257 (1990).
- [5] A. Guirao, M. Pi, and M. Barranco, *Z. Phys. D* **21**, 185 (1991).
- [6] Ph. Sindzingre, M.L. Klein, and D.M. Ceperley, *Phys. Rev. Lett.* **63**, 1601 (1989).
- [7] M.V. Rama Krishna and K.B. Whaley, *Phys. Rev. Lett.* **64**, 1126 (1990).
- [8] Y. Kwon, D.M. Ceperley, and K.B. Whaley, *J. Chem. Phys.* **104**, 2341 (1996).
- [9] D. Blume, M. Lewerenz, F. Huisken, and M. Kaloudis, *J. Chem. Phys.* **105**, 8666 (1996).
- [10] D.O. Edwards and M.S. Pettersen, *J. Low Temp. Phys.* **87**, 473 (1992).
- [11] A.F. Andreev, *Sov. Phys. JETP* **23**, 939 (1966).
- [12] D.O. Edwards and W.F. Saam, *Progress in Low Temperature Physics*, edited by D.F. Brewer (North-Holland, Amsterdam, 1978), Vol. VII A, p. 283.
- [13] J. Harms, J.P. Toennies, and F. Dalfovo, *Phys. Rev. B* **58**, 3341 (1998).
- [14] M. Barranco, M. Pi, S.M. Gatica, E.S. Hernández, and J. Navarro, *Phys. Rev. B* **56**, 8997 (1997).
- [15] S. Stringari and J. Treiner, *Phys. Rev. B* **36**, 8369 (1987).
- [16] L.B. Lurio, T.A. Rabedeau, P.S. Pershan, I.F. Silvera, M. Deutsch, S.D. Kosowsky, and B.M. Ocko, *Phys. Rev. B* **48**, 9644 (1993).
- [17] A. Sato, K. Ohishi, and M. Suzuki, *J. Low Temp. Phys.* **107**, 165 (1997).
- [18] S. Stringari and J. Treiner, *J. Chem. Phys.* **87**, 5021 (1987).
- [19] R.N. Barnett and K.B. Whaley, *J. Chem. Phys.* **99**, 9730 (1993); **102**, 2290 (1995).
- [20] S.A. Chin and E. Krotscheck, *Phys. Rev. B* **52**, 10405 (1995).
- [21] S.M. Gatica, E.S. Hernández, and M. Barranco, *J. Chem. Phys.* **107**, 927 (1997).
- [22] F. Garcias, Ll. Serra, M. Casas, and M. Barranco, *J. Chem. Phys.* **108**, 9102 (1998).
- [23] We have taken as the definition of solvation shell the region between two consecutive minima of the *total* helium density.
- [24] V.R. Pandharipande, S.C. Pieper, and R.B. Wiringa, *Phys. Rev. B* **34**, 4571 (1986).